View metadata, citation and similar papers at core.ac.uk

brought to you by CORE

provided by Archivio istituzionale della ricerca - Politecnico di Milano

PROCEEDINGS OF SPIE

SPIEDigitalLibrary.org/conference-proceedings-of-spie

Resonant micro-opto-mechanical modulators fabricated by femtosecond laser micromachining

Spagnolo, Michele, Memeo, Roberto, Motta, Riccardo, Pellegatta, Francesco, Crespi, Andrea, et al.

Michele Spagnolo, Roberto Memeo, Riccardo Motta, Francesco Pellegatta, Andrea Crespi, Roberto Osellame, "Resonant micro-opto-mechanical modulators fabricated by femtosecond laser micromachining," Proc. SPIE 11270, Frontiers in Ultrafast Optics: Biomedical, Scientific, and Industrial Applications XX, 112701B (2 March 2020); doi: 10.1117/12.2544354

SPIE.

Event: SPIE LASE, 2020, San Francisco, California, United States

Downloaded From: https://www.spiedigitallibrary.org/conference-proceedings-of-spie on 22 May 2020 Terms of Use: https://www.spiedigitallibrary.org/terms-of-use

Resonant micro-opto-mechanical modulators fabricated by femtosecond laser micromachining

Michele Spagnolo[a], Roberto Memeo[a,b], Riccardo Motta[a], Francesco Pellegatta[a,b], Andrea Crespi[a,b], and Roberto Osellame[b,a]

[a]Dipartimento di Fisica - Politecnico di Milano,
piazza Leonardo da Vinci, 32 - 20133 Milano, Italy
[b]Istituto di Fotonica e Nanotecnologie - Consiglio Nazionale delle Ricerche (IFN-CNR),
piazza Leonardo da Vinci, 32 - 20133 Milano, Italy

ABSTRACT

Integrated modulators of optical phase or intensity are essential elements to reconfigure dynamically the operation of a complex waveguide circuit, or to achieve convenient optical switching within a fiber network. Thermo-optic effects are commonly exploited to achieve dynamic phase modulation in glass-based devices, since nonlinear optical effects are weak in such substrates. Thermo-optic modulators rely on electric resistive heaters patterned on top of the waveguides: they are reliable and easy to fabricate, but they suffer from slow response, dictated by the thermal diffusion dynamics. On the other hand, optically-coupled microstructures in glass, driven at their mechanical resonances, may provide interesting possibilities to achieve modulation of the optical signals in the kilohertz range and higher. In this work, we demonstrate integrated-optics intensity modulators based on micro-cantilevers with resonant oscillation frequencies in the tens-of-kilohertz range. The mechanical structures are realized in alumino-borosilicate glass substrate by water-assisted femtosecond-laser ablation. With the same femtosecond laser an optical waveguide is inscribed within the oscillating beam; a waveguide also continues in the substrate beyond the cantilever's tip. Since the entire device, with all its optical and mechanical parts, is realized in a single fabrication process, relative alignment is guaranteed. If the cantilever is at rest, light propagating in the internal waveguide yields maximum coupling to the remaining part of the waveguide. When the device is excited at resonance by means of a piezo-electric actuator, the cantilever oscillation produces periodical variations of the coupling efficiency, with an observed contrast higher than 10 dB.

Keywords: femtosecond laser micromachining, waveguides, integrated optics modulator, resonant micro-mechanical oscillator

1. INTRODUCTION

Optical modulators and switches are fundamental components for the development of advanced fiber-optics networks or complex integrated waveguide circuits. In telecommunication applications, where fast operation frequencies are of utmost importance, optical signals are modulated up to the GHz rate, by exploiting the electro-optic effect in nonlinear substrates such as lithium niobate.[1] Carrier injection is also finding wide application in devices based on semicondutor substrates, such as silicon.[2]

However, in other scenarios, such as optical sensing or lab-on-a-chip devices,[3–5] frequency requirements may be different or anyway less stringent. On the other hand, in such contexts the operation wavelength may be critically imposed by the application: this may be incompatible with the standards of the waveguide fabrication processes in the nonlinear or semiconductor substrates mentioned above, or even fall out of their transparency windows. Chemical reactivity or toxicity of the substrate could also be an issue, when addressing chemical or biological sensing applications.

Further author information:
A.C.: E-mail: andrea.crespi@polimi.it, Telephone: +39 02 2399 6587
R.O.: E-mail: roberto.osellame@polimi.it, Telephone: +39 02 2399 6075

Frontiers in Ultrafast Optics: Biomedical, Scientific, and Industrial Applications XX, edited by Peter R. Herman, Michel Meunier, Roberto Osellame, Proc. of SPIE Vol. 11270, 112701B · © 2020 SPIE
CCC code: 0277-786X/20/$21 · doi: 10.1117/12.2544354

Downloaded From: https://www.spiedigitallibrary.org/conference-proceedings-of-spie on 22 May 2020
Terms of Use: https://www.spiedigitallibrary.org/terms-of-use

Glass materials typically present large transparency ranges, from the near infrared up to the whole visible region, have low chemical reactivity and excellent bio-compatibility. Waveguides in silica can be fabricated by conventional photolitography[6] and, as well, by direct writing techniques such as UV[7] or femtosecond laser writing.[8,9] Such waveguides also yield optimum mode-matching with optical fibers, which are indeed made of silica.

Due to the lack of nonlinearity and conductive properties, the driving technology usually employed for optical modulation in glass is thermo-optic phase-shifting. Thermo-optic phase modulators exploit the refractive index variation induced by local heating, which can be provided through electrical resistances microfabricated onto the chip. This technology is well assessed in the photolithograpy-based fabrication processes of silica-on-silicon waveguides.[6] More recently, thermo-optic phase modulators have been demonstrated also in femtosecond-laser-written waveguide circuits.[10] While a notable level of complexity can be reached, with many actuators on the same chip,[11–13] the main limitation of these devices certainly resides in their slow response times, which are governed by the thermal diffusion dynamics and are hardly below the millisecond range.

In this work, we propose and demonstrate an optical-intensity modulator, integrated in a glass chip. The device is entirely fabricated by femtosecond laser pulses and is based on a microstructured cantilever that contains an optical waveguide. The optical waveguide continues in the substrate beyond the cantilever's tip. When a piezo-actuator induces the resonant oscillation of the cantilever (which is in the range of the tens of kilohertz), the optical transmission from one waveguide segment to the other is modulated with high contrast at double of the oscillation frequency.

2. MATERIALS AND METHODS

The device is entirely realized by Femtosecond Laser Micromachining in a commercial alumino-borosilicate glass substrate (Eagle XG, Corning). This material has density ρ =2380 kg/m^3 and Young modulus E = 73.6 GPa.

We employ a compact fiber-based Ytterbium laser source (Amplitude Satsuma), delivering pulses of 250 fs duration and $>$ 10 μJ energy at repetition rates up to 1 MHz. Femtosecond laser pulses are focused into the substrate by a 20X water-immersion objective (Zeiss N-Achroplan). Relative translation between the sample and the laser focus is provided by a high-precision three-axis system (Aerotech ANT); in particular, the glass sample is mounted on a XY stage that provides the motion in the horizontal plane, while the focusing objective is mounted on a vertical stage.

Microstructuration of the cantilever was performed by Water Assisted Laser Ablation, starting the irradiation from bottom surface. The structure was divided into box-shaped sections and, to excavate each region, only the external surfaces were processed. Irradiation parameters for ablation were 50 kHz repetition rate, translation speed of 2 mm/s and pulse energy of 1.8 μJ.

Waveguides are fabricated by a single linear laser scan, at 150 μm height from the bottom surface. Irradiation parameters were chosen to achieve single-mode operation at 1.55 μm wavelength, together with low propagation loss ($\sim$0.88 dB/cm) and mode dimension similar to that of standard optical fibers ($\sim$13 μm $1/e^2$ diameter). In particular, 350 nJ laser pulses at 1 MHz repetition rate were employed, while the sample was translated at uniform speed of 10 mm/s.

Waveguide inscription and microstructuring by ablation were performed in the same fabrication session, thus guaranteeing perfect relative alignment. After laser processing, an ultrasound bath was used to facilitate debris removal from the ablated cavities. Finally, a standard single-mode optical fiber is accurately aligned to the input waveguide of the device, using a 6-axis hexapod system (H-811 Physik Instrumente). Coupling between the fiber and the waveguide is then made permanent using optical-quality UV-curing resin.

To characterize the device operation, the glass sample is clamped between a piezo-actuator and an elastic support, so that the whole device can oscillate in the plane of the lowest-order natural mode of the cantilever. To drive the piezo-actuator, the output signal from a function generator (Tektronix AFG3011C) is voltage amplified by an inductive transformer: in this way, the 20 V peak-to-peak provided by the function generator can be multiplied up to about 120 V peak-to-peak. Coherent light from a laser diode, emitting at 1.55 μm wavelength, is coupled into the input fiber of the device. The output light is collected by an aspheric lens and focused onto

Downloaded From: https://www.spiedigitallibrary.org/conference-proceedings-of-spie on 22 May 2020
Terms of Use: https://www.spiedigitallibrary.org/terms-of-use

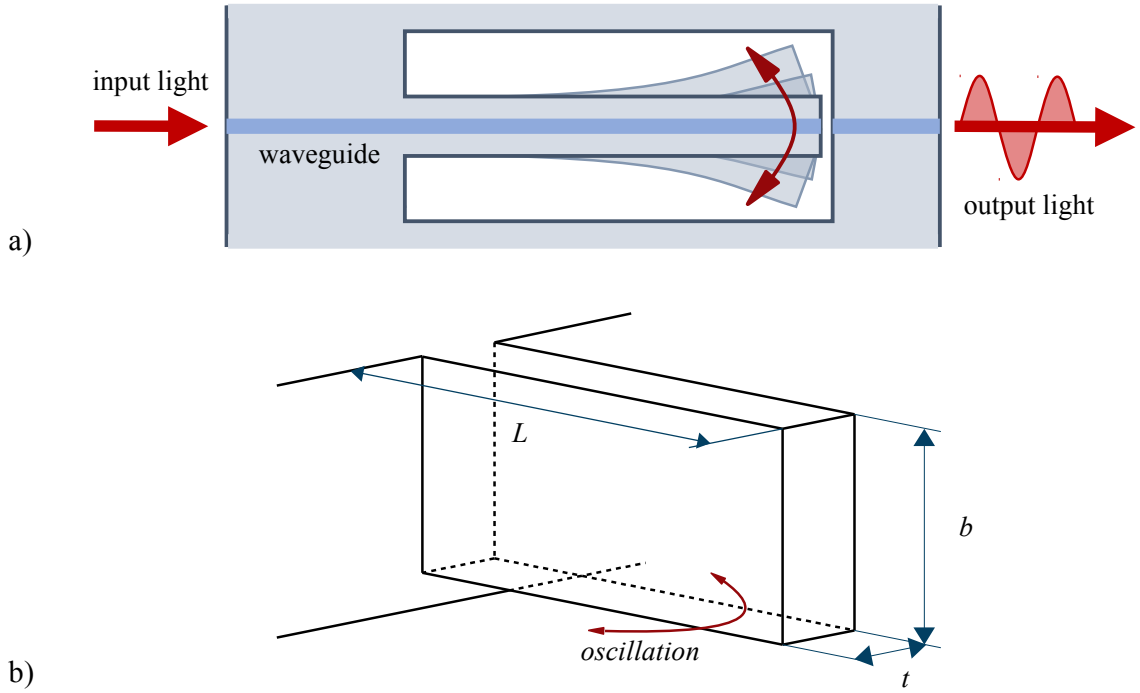

Figure 1. a) Working principle of the intensity modulator. When the device is at rest, the waveguide in the cantilever is aligned with the one in the bulk, separated by a small gap as shown in. During the oscillation the two waveguide misalign with each other. b) Dimensional scheme of the cantilever structure.

a 10-MHz-bandwidth InGaAs photodiode, provided with amplification electronics. The driving voltage from the function generator and the signal from the photodiode are simultaneously monitored with a 200-MHz-bandwidth oscilloscope (Tektronix DPO2024B).

3. THEORY OF OPERATION

The device basically consists in a cantilever structure with an embedded optical waveguide, as in Figure 1. The main idea is to drive the oscillation of the cantilever at one of its natural frequencies, so that the output port of the embedded waveguide (placed on the cantilever's tip) is periodically displaced from input port of the waveguide segments continuing in the substrate, thus providing a modulation of the optical transmission due to lateral misalignment.

By assuming Gaussian optical modes of the propagating light, both when it is guided in the waveguides and when it is travelling in free-space between the tip of the cantilever and the wall of the substrate, it is possible to derive a simple analytical expression for the transmitted signal, as a function of the cantilever deformation. In particular, if the displacement of the cantilever's tip is much smaller than its length, we may neglect tilt angles in the free space propagation and the device transmission T is given by the overlap integral between two Gaussian modes laterally displaced by d, which is the displacement of the cantilever's tip from its equilibrium position.

$$T(d) = e^{-\frac{d^2}{\sigma^2}} \tag{1}$$

If we neglect also the divergence of the beam in the free-space propagation region, σ is equal to the waveguide mode radius, which is also equal to the beam waist of the free-space Gaussian beam.

The oscillation of the cantilever is well described using the analytical beam theory by Euler. The resonance frequencies of a cantilever with a rectangular cross-section are given by:

$$\nu_n = R_n^2 \frac{\pi t}{4L^2} \sqrt{\frac{E}{3\rho}} \tag{2}$$

Downloaded From: https://www.spiedigitallibrary.org/conference-proceedings-of-spie on 22 May 2020
Terms of Use: https://www.spiedigitallibrary.org/terms-of-use

	$L = 1.0$ mm		$L = 1.2$ mm		$L = 1.5$ mm	
Mode order	f_{meas} [kHz]	f_{theo} [kHz]	f_{meas} [kHz]	f_{theo} [kHz]	f_{meas} [kHz]	f_{theo} [kHz]
1	35.9	35.9	23.8	23.7	16.1	16.0
2	223	225	149	149	101	100

Table 1. Measured and theoretical resonance oscillation frequencies, for cantilevers of different length L. Values for the first-order and second-order modes are reported. The theoretical values are calculated by substituting actual dimensions of the fabricated cantilevers (as measured by an optical microscope) in Eq. (2).

where L is the length of the cantilever, t is the thickness (parallel to the direction of oscillation), ρ is the material density and E is the Young modulus. The coefficients R_i are numerically evaluated and for the two lowest-order modes are $R_1 \simeq 0.597$ and $R_2 \simeq 1.494$.

In our experiments the cantilever is actuated by forcing an oscillation of the fixed base. If we consider the transfer function of the externally-imposed sinusoidal displacement to the displacement of the cantilever's tip, the mechanical system has the same linear behaviour of a damped mass-spring harmonic oscillator.[14] Within this analogy the equivalent cantilever stiffness is $k_{eq} = \frac{1}{4} E\, b\, t^3 / L^3$ and its equivalent mass is $m_{eq,n} = 3\rho\, b\, t\, L/(\pi R_n)^4$; in the latter formulas, b is the width of the cantilever, measured transversally to the oscillation direction. Note that $m_{eq,n}$ depends on the mode order n; in the case of the first mode, $m_{eq,1} \sim 0.24\, \rho\, b\, t\, L$. The transfer function thus simply reads:

$$T(\omega) = \frac{\omega^2}{-\omega^2 + 2j\xi\Omega\omega + \Omega^2} \tag{3}$$

where $\Omega = \sqrt{\dfrac{k_{eq}}{m_{eq,n}}}$ is the resonant angular frequency and ξ is a damping term. In general both internal friction, due to the material viscosity, and external friction, due to the viscosity of the surrounding medium (i.e., friction with the air), can play a role in damping the cantilever oscillations. For cantilevers comparable to ours in size, and immersed in air at ambient pressure, damping is mainly due to air friction.

Note that, at resonance ($\omega \sim \Omega$), the transfer function reduces to $T \simeq 1/(2j\xi)$. Its modulus coincides with the so-called quality factor:

$$Q = \frac{1}{2\xi} \tag{4}$$

The quality factor is thus the multiplication factor between the oscillation amplitude imposed to the whole device by the piezo-actuator and the actual oscillation amplitude of the cantilever's tip.

4. EXPERIMENTAL RESULTS

Several different cantilever devices were fabricated, with nominal dimensions $t = 50$ μm, $b = 250$ μm and L spanning from 700 μm to 1.5 mm. The large difference between the design thickness and height is chosen to separate in frequency the in-plane modes of oscillation from the off-plane modes. Due to fabrication tolerances, the thickness of the fabricated cantilevers was actually reduced to about $t \simeq 40$ μm and their height resulted to be about 240 μm. The gap between the tip and the rest of the substrate was typically around 15 μm: the presence of this gap is the main cause of optical insertion loss of this kind of device, which are about 8 dB in the conditions of maximum transmission.

As a first characterization measurement, the frequency of the sinusoidal driving signal from the function generator was scanned from a few kilohertz up to 1 MHz, while keeping a sufficiently high (∼20 V peak-to-peak) signal amplitude. Frequencies that are associated to non-negligible and synchronous modulations of the optical signal at the output correspond to resonant oscillation modes of the cantilever. The observed resonance frequencies show good agreement with theoretical predictions from Eq. (2) (see Table 1).

As a second measurement, we characterized the modulation of the optical signal, as a function of the amplitude of the driving electrical signal, at the frequency corresponding to the first resonant mode. In detail, the function

Downloaded From: https://www.spiedigitallibrary.org/conference-proceedings-of-spie on 22 May 2020
Terms of Use: https://www.spiedigitallibrary.org/terms-of-use

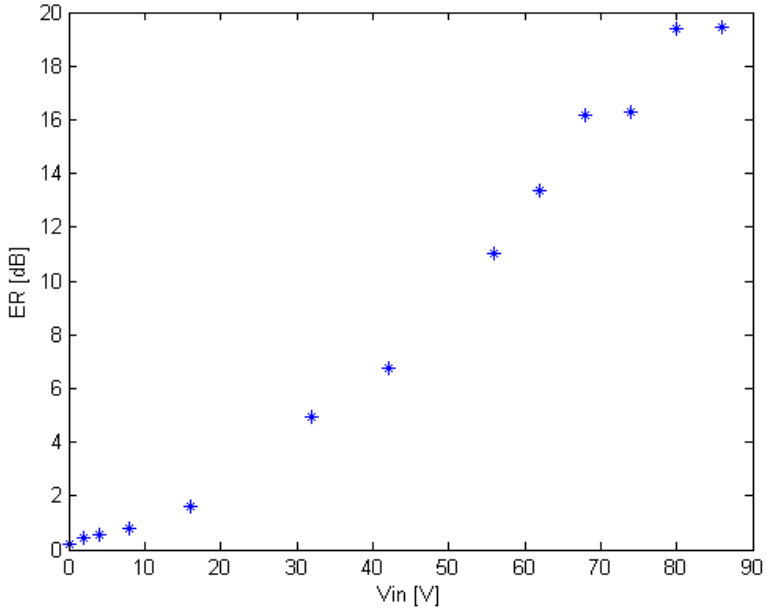

Figure 2. Measured E.R. for different peak-to-peak voltages applied to the piezo-electric actuator.

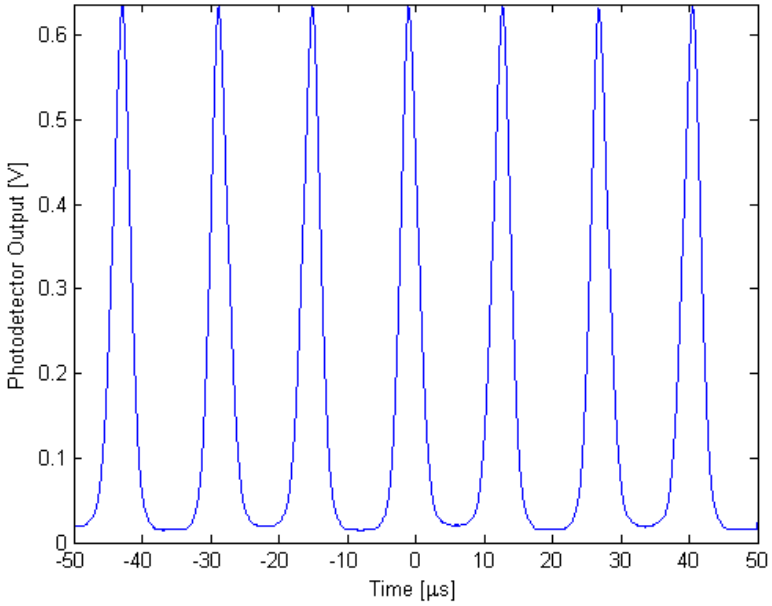

Figure 3. Measured signal at the photodetector when a 86-V peak-to-peak sinusoid is applied to the piezo-electric actuator, for a 1.0 mm long cantilever. An optical pulse-train is observed at 71.8 kHz frequency. High-frequency noise was digitally filtered from the signal.

generator was set to produce a sinusoid at the resonance frequency and the peak-to-peak amplitude of the signal was varied from 0 V to 86 V. At each voltage step the trace on the oscilloscope was recorded.

Figure 3 shows an example of acquired signal from the photodiode. One can note that the optical modulation occurs at a frequency that is twice the one of the mechanical oscillation of the cantilever; in fact, the cantilever's tip crosses its "rest" position twice in each oscillation period.

Downloaded From: https://www.spiedigitallibrary.org/conference-proceedings-of-spie on 22 May 2020
Terms of Use: https://www.spiedigitallibrary.org/terms-of-use

As a significant figure of merit, one can define the Extinction Ratio (E.R.) as:

$$\text{E.R.}|_{\text{dB}} = 10\log_{10}\frac{V_{max}}{V_{min}} = 10\log_{10}\frac{P_{max}}{P_{min}} \tag{5}$$

where V_{min} and V_{max} are the minimum and maximum voltages of the photodiode signal, as measured on the oscilloscope. These are directly proportional to the minimum and maximum of the transmitted optical power (P_{min} and P_{max}, respectively).

Figure 3 reports the measured E.R. as a function of the peak-to-peak signal amplitude on the piezo-actuator, for the cantilever with $L = 1.0$ mm. These results show that the E.R increases with the signal amplitude and exceeds 19 dB for a 86 V peak-to-peak driving sinusoid.

We also performed a more detailed characterization of the transfer function Eq. (3) around the frequency of the first in-plane mode. The driving voltage of the piezo-electric actuator was fixed to 38.4 V peak-to-peak, while sweeping the frequency of the sinusoidal signal around the resonance peak. From the measured $\frac{V_{max}}{V_{min}}$ ratio, at each frequency, one can recover the maximum displacement d of the cantilever's tip by inverting Eq. 1. Figure 4 plots the maximum displacement as a function of the frequency, around the resonance peak, for the same structure of Fig. 3. By fitting a function with the form (3) on the experimental data, it is also possible to retrieve the quality factor of the resonant structure, which in this case is measured as high as 468.

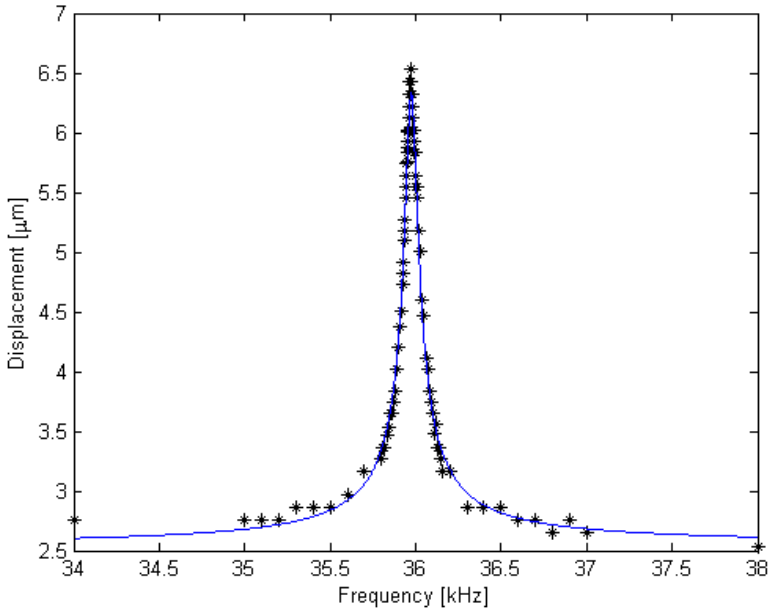

Figure 4. Maximum displacement of the cantilever's tip in each oscillation cycle, as retrieved from the measured modulation of the optical signal. Black stars are experimental points, while the continuous line is a best-fit of a function with the form (3), properly normalized.

5. DISCUSSION AND CONCLUSION

We have demonstrated a micro-mechanical optical modulator, entirely fabricated with femtosecond laser pulses in glass. The device is based on an oscillating cantilever, with length in the order of 1 mm and cross section of about $\sim 50 \times 250\ \mu\text{m}^2$. The resonance frequency can be tuned in the tens-of-kilohertz range by varying the length of the structure. As discussed, the modulation of the optical signal occurs at twice the frequency of the mechanical oscillation.

We have shown a modulation of the optical signal with E.R. larger than 19 dB, at a frequency of ~ 72 kHz. This well overcomes the limits of glass-based modulators that rely on the thermo-optic effect.

Downloaded From: https://www.spiedigitallibrary.org/conference-proceedings-of-spie on 22 May 2020
Terms of Use: https://www.spiedigitallibrary.org/terms-of-use

The operation wavelength of the devices shown here falls in the telecom range. However, the femtosecond laser writing technology easily allows to fabricate single-mode waveguides for arbitrary wavelengths in the visible or near-infrared regions, provided that the irradiation parameters are properly tuned.[10,13,15] In addition, the possibility of realizing optofluidic structures in EagleXG borosilicate glass, by femtosecond-laser micromachining, has been recently demonstrated.[16]

In perspective, this device could be included in a more complex network of waveguide or fiber components. In particular, it could act as integrated intensity modulator, embedded within a lab-on-chip device. Furthermore, oscillating resonant structures similar to the one reported here, but immersed in liquid, might also be employed as viscosity sensors for the surrounding fluid.

ACKNOWLEDGMENTS

This work was supported by the European Research Council (ERC) Advanced Grant CAPABLE (grant agreement no. 742745).

REFERENCES

[1] Liu, K., Ye, C. R., Khan, S., and Sorger, V. J., "Review and perspective on ultrafast wavelength-size electro-optic modulators," *Laser & Photonics Reviews* **9**(2), 172–194 (2015).

[2] Reed, G. T., Mashanovich, G., Gardes, F. Y., and Thomson, D., "Silicon optical modulators," *Nature photonics* **4**(8), 518 (2010).

[3] Kuswandi, B., Huskens, J., Verboom, W., et al., "Optical sensing systems for microfluidic devices: a review," *Analytica chimica acta* **601**(2), 141–155 (2007).

[4] Li, C., Bai, G., Zhang, Y., Zhang, M., and Jian, A., "Optofluidics refractometers," *Micromachines* **9**(3), 136 (2018).

[5] Wang, N., Dai, T., and Lei, L., "Optofluidic technology for water quality monitoring," *Micromachines* **9**(4), 158 (2018).

[6] Takato, N., Jinguji, K., Yasu, M., Toba, H., and Kawachi, M., "Silica-based single-mode waveguides on silicon and their application to guided-wave optical interferometers," *Lightwave Technology, Journal of* **6**, 1003–1010 (Jun 1988).

[7] Svalgaard, M., Poulsen, C., Bjarklev, A., and Poulsen, O., "Direct uv writing of buried singlemode channel waveguides in ge-doped silica films," *Electronics Letters* **30**(17), 1401–1403 (1994).

[8] Gattass, R. and Mazur, E., "Femtosecond laser micromachining in transparent materials," *Nature Photonics* **2**(4), 219–225 (2008).

[9] Osellame, R., Cerullo, G., and Ramponi, R., [*Femtosecond laser micromachining: photonic and microfluidic devices in transparent materials*], vol. 123, Springer Science & Business Media (2012).

[10] Flamini, F., Magrini, L., Rab, A. S., Spagnolo, N., D'Ambrosio, V., Mataloni, P., Sciarrino, F., Zandrini, T., Crespi, A., Ramponi, R., and Osellame, R., "Thermally reconfigurable quantum photonic circuits at telecom wavelength by femtosecond laser micromachining," *Light: Science & Applications* **4**, e354 (2015).

[11] Carolan, J., Harrold, C., Sparrow, C., Martín-López, E., Russell, N. J., Silverstone, J. W., Shadbolt, P. J., Matsuda, N., Oguma, M., Itoh, M., et al., "Universal linear optics," *Science* **349**(6249), 711–716 (2015).

[12] Dyakonov, I., Pogorelov, I., Bobrov, I., Kalinkin, A., Straupe, S., Kulik, S., Dyakonov, P., and Evlashin, S., "Reconfigurable photonics on a glass chip," *Physical Review Applied* **10**(4), 044048 (2018).

[13] Polino, E., Riva, M., Valeri, M., Silvestri, R., Corrielli, G., Crespi, A., Spagnolo, N., Osellame, R., and Sciarrino, F., "Experimental multiphase estimation on a chip," *Optica* **6**, 274–279 (2019).

[14] Lee, J.-H., Lee, S.-T., Yao, C.-M., and Fang, W., "Comments on the size effect on the microcantilever quality factor in free air space," *J. Micromech. Microeng.* **17**(139) (2007).

[15] Douglass, G., Dreisow, F., Gross, S., and Withford, M., "Femtosecond laser written arrayed waveguide gratings with integrated photonic lanterns," *Optics express* **26**(2), 1497–1505 (2018).

[16] Crespi, A., Osellame, R., and Bragheri, F., "Femtosecond-laser-written optofluidics in alumino-borosilicate glass," *Optical Materials: X* **4**, 100042 (2019).

Downloaded From: https://www.spiedigitallibrary.org/conference-proceedings-of-spie on 22 May 2020
Terms of Use: https://www.spiedigitallibrary.org/terms-of-use